DOI: 10.48011/asba.v2i1.1305

Comparison of Nonlinear Receding-Horizon and Extended Kalman Filter Strategies for Ground Vehicles Longitudinal Slip Estimation

Elias Dias Rossi Lopes*, Gustavo Simão Rodrigues and Helon Vicente Hultmann Ayala***

**Pontifícia Universidade Católica do Rio de Janeiro, Rio de Janeiro, Brasil*
(e-mails: elias.rossi@gmail.com, helon@puc-rio.br)
*** Instituto Militar de Engenharia, Rio de Janeiro, Brasil*
(e-mail: simao@ime.eb.br)

Abstract: Friction efforts are present in almost all mechanical applications, due to contact between bodies and there are many important situations, in which they must be properly controlled. Among these, there are tire contact forces, which is focus of many studies in autonomous vehicles and control applications on vehicle systems, since the tire forces and moments are nonlinear and may be modelled as friction efforts. Any control synthesis focused to optimize its performance must be associated to state estimators, since the efforts depend on slip variables, as longitudinal slip and sideslip angle, and it is not possible to accurately measure them. So, in this paper, two state estimation algorithms are evaluated: Extended Kalman Filter (EKF) and Moving Horizon State Estimation (MHSE), which are applied to a quarter-car model for longitudinal dynamics. It is presented that, for both traction and braking phases, the MHSE is more accurate, since it takes explicitly into account the nonlinear model in the estimation process, independently of Jacobian sensitivities to discontinuities as is the case here. So, it is demonstrated that the developed estimator may be successfully associated to controllers with the objective of optimize tire performance in traction and braking control.

Keywords: Extended Kalman Filter, Moving Horizon State Estimation, Tire Dynamics, Nonlinear Efforts, Ground Vehicles

1. INTRODUCTION

In many mechanical applications, friction interactions are commonly found, once there is usually contact between bodies. In most cases, these interactions have a nonlinear nature, which difficult any attempt of control the system performance or mitigating their effects, when harmful. Coulomb friction, tire-road forces in vehicles and bit-rock interaction on perforation process are some examples of these effects.

However, in a control application, it is not common to be possible to measure all states or all controlled variables. In these situations, it is usually used a state observer, which has as function estimate the states based on the measured variables. Among the state estimation algorithms, the Kalmar is one of the most known, such as one of its versions applied to nonlinear systems, the Extended Kalman Filter (EKF). On last decades, other algorithms have been developed, looking for more robustness and accuracy. The Moving Horizon Estimation (MHE) is one of these, defined by Alessandri et al. (2008) as a powerful and robust approach, suitable in systems with modelling uncertainties and numerical errors. It was developed as a dual of Model Predictive Control and estimates the states variables using a defined horizon of recent information and measures. These algorithms are studied in many different applications (Brembeck, 2019), so that it is possible to clearly understand its power and robustness.

In vehicle systems, nonlinear observers are implemented on many control applications, but we may specially remark those dependents on tire dynamics, such as braking, traction and stability control. In most applications, the controlled variables, usually longitudinal slip, attitude angles, sideslip angle and others are impossible to measure, which justifies the implementation of observer-based control.

In this context, Zareian et al. (2015) propose the use of EKF associated to Recursive Least Squares and Neural Networks in a methodology of estimation of road friction coefficient, which is a hardly obtaining parameter. Kayacan et al. (2018) present a control strategy for tracked field robots with receding horizon estimation and control (RHEC). The estimation algorithm is used for estimate states and parameters, and the receding horizon control is based on an adaptive system whom model is time varying. Li et al. (2014) present an EKF based estimator for sideslip angle for a vehicle stability control and the authors remark that its measure is complex and expensive, which justifies the estimation process. Sun et al. (2014) apply a nonlinear observer for state estimation on an ABS, due to nonlinearity of the friction force during brake.

Boada et al. (2017) develop a new method for estimation of different states and parameters of a vehicle, using a constrained version of Kalman Filter to consider the physical limitations of the parameters. It is demonstrated by experimental results that the constraints are important to improve accuracy of the algorithm. Na et al. (2018) present two torque estimation methods for vehicle engines, using a proper dynamical model and air mass flow rate and engine speed, which are measurable. Jo et al. (2016) present a road slope and position estimator, which inputs are GPS data and vehicle onboard sensors. The estimator proposed presents more accurate and reliable results, which is proven by experiments. Hsiao (2012) proposes an observer-based control scheme for traction force, robust to variations on road conditions and uncertainties on tire models.

Nilsson et al. (2014) study the problem of estimating position and direction of a vehicle with a single camera since it is hardly dependent of image quality. So, the authors propose an estimator which combines onboard vehicle sensors and adjusted camera images, with a single-track model. Chen et al. (2011) remark the importance of tire-road friction coefficient estimation for autonomous vehicle applications and present an observer which does not depend on longitudinal motion information and is properly associated to an adaptive speed control. Singh et al. (2013) remark that simpler stability control performs well in many situations, but it is improved when a tire-road friction estimator is associated to the control scheme. In this way, the authors present a method in which is used frequency response of tire vibrations on the estimation algorithm. Hsu et al. (2009) remark the importance of knowledge of physical limits of parameters used on vehicle control, such as tire slip angle and maximum lateral force and propose a model-based estimation algorithm that estimates them using information from the applied steering torque.

Du et al. (2015) construct a side-slip estimator based on a fuzzy system for lateral dynamics and the nonlinear Dugoff tire model, using measured yaw rate and estimated states. Li et al. (2019) use the same tire model to propose a side-slip estimation algorithm robust to inaccurate tire parameters.

Recent research in vehicle control point the increased use of electric in-wheel motors, which allows many control strategies and simpler configurations of electric vehicles. These devices allow to reduce mass and to simplify transmission system, which is favorable in electric and autonomous vehicles. Zhao and Liu (2014) present a four degree-of-freedom nonlinear dynamical model of a four independent wheel electric vehicle, considering the measurements provided by modern sensors used on vehicles. An observer is associated to this model to estimate vehicle velocity and roll angle, since these variables must be controlled on stability control system. Feng et al. (2020) present two estimation algorithms based on moving horizon methods. The observer is applied on a four wheels electric robotic platform on different friction conditions.

Jeon et al. (2018) propose a real-time constrained Kalman filter algorithm for estimation of the three tire forces on vehicle tires, namely, vertical, longitudinal and lateral forces in mobile robots equipped with wheel encoders and navigation sensors. Tire forces in the estimation process are modeled by Magic Formula, an empirical model developed by Pacejka (1992). Hong et al. (2014) present an application of Unscented Kalman Filter to estimation of inertial parameters of vehicles, which may be not accurately determined in design phase. Heidfeld et al. (2019) applied the same algorithm in a state and tire slip estimation for an electric vehicle with four independent wheels.

Estimation algorithms are used also in path-tracking applications for autonomous vehicles. Brembeck (2019) remarks that state-estimators for autonomous vehicles are even more challenging, since the complexity of models and applications rises along the time. In this way, he presents a vehicle state observer to estimate position, yaw angle and their rates, with focus on path following and he discuss about the balance between model complexity and estimator performance. The author uses constrained versions of EKF and MHSE to better approximate the results to real data. Jalali et al. (2017) present a model predictive control scheme for tracking yaw rate with small lateral velocity and tire slips. The proposed method controls lateral velocity adjusting reference yaw rate, which reduces the size of model and computational complexity. They also present an estimation algorithm by means of vehicle kinematics and tire model.

The state estimation is possible only if the system is fully observable. The condition of observability of a system is characterized by the possibility of observe all state variables by means of the measurement variables, or yet, if two different sets of states are related to two different sets of measured variables (Kou et al., 1973). The authors explore the observability of nonlinear systems, presenting two sufficient conditions to prove it. Katriniok and Abel (2015) present an EKF estimation for longitudinal and lateral velocities and yaw rate. They also present an approach for evaluate local observability online and a virtual measurement variable for instants in which local observability is lost.

In this context, this work aims to present a comparative analysis between EKF and MHSE for estimation of longitudinal slip in ground vehicle control applications. We may observe on the literature review that the MHSE is not exploited on vehicle systems, and thus the main goal of the paper is to assess its performance in such applications. Both estimators are applied in the same conditions to estimate states of longitudinal dynamics of a quarter-car model, actuated by a braking or traction torque in the case of an in-wheel motor. In the estimation process, the state estimation algorithms are employed to estimate accurately the longitudinal slip and velocity of the vehicle. We observe in the literature review that the comparison has not been assessed thus far in such application, even if results in the literature show overall better results for the receding-horizon approaches (Alessandri et al., 2008). It is important to remark that the longitudinal slip is important for traction and braking control strategies. The present paper aims at the evaluation of the performance of MHSE and EKF, their limitations and advantages, aiming at future control application on autonomous vehicles. The present work shows overall favourable results for the MHSE approach, despite its greater computational effort.

At first, it is presented the theoretical basis of quarter-car longitudinal dynamic model, studying the longitudinal force formulations and the parameters employed. In the following section, the estimation processes, namely, the Extended Kalman Filter and the Moving Horizon State Estimation are defined, and their algorithms and evaluation metrics are presented. Then, it is demonstrated the data obtaining by means of a simulation with noisy measured variables and the results of the estimation process. Finally, the conclusions are commented, evaluating both estimators, and presenting the possibilities of future research.

2. QUARTER-CAR DYNAMIC MODEL

A quarter-car model may be effectively used for the study of nonlinear estimation. In this model, the vehicle is understood as a concentrated mass (with mass *m*) over a single wheel (with moment of inertia *J*), and there are no effects related to vertical or lateral dynamics. Are considered also the rolling resistance momentum and aerodynamic resistance (Figure 1).

The first one affects the wheel dynamics and it is due to energy dissipation in the tire structure and rubber (Jazar, 2017). Mathematically, it may be described as proportional to normal load, according to the coefficient f_R. The drag force acts on vehicle gravity center and is due to aerodynamic efforts. For simplification, we must assume that it is proportional to the square of longitudinal velocity according to *C*. So, the dynamic equations of the system are:

$$m\dot{v} = F_x - R_{Aer} = F_x - Cv^2 \quad (1)$$

$$J\dot{\omega} = T - rF_x - M_{Rol} = T - rF_x - rf_R mg \quad (2)$$

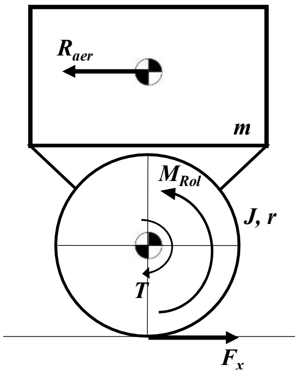

Figure 1: Schematic model of quarter car

In the wheel dynamic equation, T is the torque, which is considered the system input. The traction force F_x is defined as proportional to the normal load (in the quartel-car model defined as the weight) according to a factor μ (Savaresi, 2005). Then, treating $c = C/m$, the motion equations may be written as:

$$\dot{v} = \mu(\lambda)g - cv^2 \quad (3)$$

$$\dot{\omega} = \frac{T}{J} - (\mu(\lambda) + f_R)\frac{mgr}{J} \quad (4)$$

The friction coefficient μ depends on the longitudinal slip λ, which may be define as:

$$\lambda = \frac{\omega r - v}{v} = \frac{\omega r}{v} - 1 \quad (5)$$

We may note that during an acceleration, slip is positive, and during braking, it is negative and equation (5) demonstrate that λ must be on [-1,∞[. There are many formulations for the relationship between μ and λ, as the Julien Theory (Lopes et al., 2019), the Burckhardt model (Savaresi, 2005) and the Magic Formula (Pacejka, 1992). All of them depends on many parameters, which are empirically obtained. The last one has the advantage of being continuous in whole domain of slip, which does not happen on the others, reducing elapsed time of simulations and estimation processes. So, according to the Magic Formula model, μ may be written as:

$$\mu(\lambda) = A\sin\big(B\,\mathrm{atan}\big(C\lambda - D(C\lambda - \mathrm{atan}(C\lambda))\big)\big) \quad (6)$$

The parameters A, B, C and D depends on road conditions on which the vehicle moves. Figure 2 presents the curves associated to many road conditions, which are obtained by approximation to data presented by Savaresi (2005).

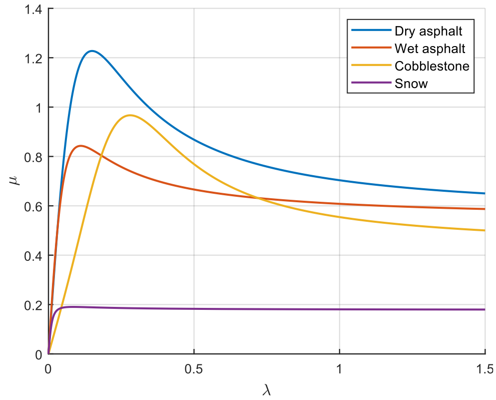

Figure 2: Friction coefficients for different pavements.

Furthermore, we must define the longitudinal slip and the velocity as states of the system, since they are controlled variables on many applications, and the tire angular velocity as the output variable, since it is usually measured. In this way, from equation (5), the ω must be written in terms of *v* and λ (equation (7)) and we may obtain its time derivative (equation (8)).

$$\omega = \frac{v(1+\lambda)}{r} \quad (7)$$

$$\dot{\omega} = \frac{\dot{v}(1+\lambda) + \dot{\lambda}v}{r} \quad (8)$$

Generally, we may define a nonlinear state space model as:

$$\begin{cases} \dot{\boldsymbol{x}} = f(\boldsymbol{x},\boldsymbol{u}) \\ \boldsymbol{z} = h(\boldsymbol{x},\boldsymbol{u}) + \boldsymbol{\xi}_n \end{cases} \quad (9)$$

In equation (9), $\boldsymbol{x}$ is the vector of states, $\boldsymbol{u}$ the input of the system, $\boldsymbol{z}$ are the outputs, that is, the measured states and $\boldsymbol{\xi_n}$ is a white measurement noise, which may be considered on simulation process and data obtaining. Substituting equation (8) on (4), we obtain the nonlinear state space equations of the system.

$$\dot{\lambda} = \frac{Tr}{Jv} - \frac{(1+\lambda)}{v}(\mu(\lambda)g - cv^2) - (\mu(\lambda) + f_R)\frac{mgr^2}{Jv} \quad (10)$$

$$\dot{v} = \mu(\lambda)g - cv^2 \quad (11)$$

$$\omega = \frac{v(1+\lambda)}{r} \quad (12)$$

For Kalman filter application, it was remarked that the Jacobians of the nonlinear model should be defined. These

Jacobians correspond, respectively, to state and output matrices of a linear state space model. For longitudinal dynamics, they are:

$$\boldsymbol{F} = \frac{\partial \boldsymbol{f}}{\partial \boldsymbol{x}} = \begin{bmatrix} \frac{\partial \dot{\lambda}}{\partial \lambda} & \frac{\partial \dot{\lambda}}{\partial v} \\ \frac{\partial \dot{v}}{\partial \lambda} & \frac{\partial \dot{v}}{\partial v} \end{bmatrix} \tag{13}$$

$$\boldsymbol{H} = \frac{\partial \boldsymbol{h}}{\partial \boldsymbol{x}} = \begin{bmatrix} \frac{\partial \omega}{\partial \lambda} & \frac{\partial \omega}{\partial v} \end{bmatrix} = \begin{bmatrix} \frac{v}{r} & \frac{1+\lambda}{r} \end{bmatrix} \tag{14}$$

As mentioned on the previous section, the estimation of all states is possible if, and only if, the system is full observable. Specifically on the quarter car model, we may calculate the observability matrix based on the Jacobians of the nonlinear model, with the classical observability matrix, defined as:

$$\mathcal{O} = \begin{bmatrix} H \\ HF \end{bmatrix} \tag{15}$$

On the simulation process, it is possible to note that the observability matrix has full rank in all time. Consequently, all states are observables and, in a first analysis, both estimation algorithms may be successfully employed.

3. STATE ESTIMATION METHODS

In a control application, it is not possible to always measure all states of the system. In these cases, an estimator must be defined, with the objective of estimate all states in each instant, based on output variables, that is, the measured ones. The existence of an estimator is conditioned to the observability of the system, which indicates that all states may be observed by means of the output variables.

In this work, two methods are explored: Extended Kalman Filter (EKF) and the Moving Horizon State Estimation (MHSE). The Extended Kalman Filter is one of nonlinear applications of the Kalmar Filter, developed for linear systems (Bar-Shalom et al., 2004).

The EKF is applied to a discrete-time system, such as:

$$\begin{cases} \boldsymbol{x}(i+1) = \boldsymbol{f}(\boldsymbol{x}(i), \boldsymbol{u}(i)) \\ z(i+1) = \boldsymbol{h}(\boldsymbol{x}(i+1)) \end{cases} \tag{16}$$

Briefly, the algorithm for EKF is described on the sequence below, for a state estimate ($\hat{x}(i|i)$), that is the system state at sample *i*, estimated on sample *i*. It is important to remark that the matrices P, R and Q must be initialized as diagonal types, with large traces, to assure the convergence of the filter.

1. Jacobians:

$$F(i) = \frac{\partial f}{\partial x}_{x=\hat{x}(i|i)} \tag{17}$$

$$H(i) = \frac{\partial h}{\partial x}_{x=\hat{x}(i|i)} \tag{18}$$

2. State prediction covariance:

$$P(i+1|i) = F(i)P(i|i)F(i)^T + Q(i) \tag{19}$$

3. Residual covariance

$$S(i+1) = R(i) + H(i)P(i+1|i)H(i)^T \tag{20}$$

4. Filter gain

$$W(i+1) = P(i+1|i)H(i)^T S(i+1)^{-1} \tag{21}$$

5. State prediction

$$\hat{x}(i+1|i) = f(\hat{x}(i|i), u(i)) \tag{22}$$

6. Measurement prediction

$$\hat{z}(i+1|i) = h(\hat{x}(i+1|i)) \tag{23}$$

7. Measurement residual

$$\nu(i+1) = z(i+1) - \hat{z}(i+1|i) \tag{24}$$

8. Updated state estimate

$$\hat{x}(i+1|i+1) = \hat{x}(i+1|i) + W(i+1)\nu(i+1) \tag{25}$$

9. Updated state covariance

$$P(i+1|i+1) = P(i+1|i) - W(i+1)S(i+1)W(i+1)^T \tag{26}$$

The MHSE is most recent and have its development related to Model Predictive Control, since there is a duality between regulation and estimation processes (Alessandri, 2008). In this method, the estimation of states in each instant of time is obtained by means a prediction of the states N instants before and the estimation of the states in this window of time using the dynamic model and the measured data. In this case, continuous or discrete-time models may be used. The algorithm of MHSE is:

1. Prediction of states at *t-N*

$$\bar{x}(t-N|t) = f(\hat{x}(t-N-1|t-1), u(t-N-1)) \tag{27}$$

2. State estimation at *t-N*

$$\hat{x}(t-N|t) = argmin\left(\mu\|\hat{x}(t-N|t) - \bar{x}(t-N|t)\| + \sum_{i=t-N}^{t} \|h(\hat{x}(i|t)) - z(i)\|\right) \tag{28}$$

3. State estimation at the horizon

$$\hat{x}(i+1|t) = f(\hat{x}(i|i), u(i)) \quad i = t-N, \ldots, t-1 \tag{29}$$

4. State estimation at *t*

$$\hat{x}(t|t) = f(\hat{x}(t-1|t), u(t-1)) \tag{30}$$

On the algorithm, it is important to remark some observations. The first one is related to the parameter μ, which indicates the confidence on the state prediction, that is, with this parameter, it may be differently considered the dynamic model and state prediction or the measured data, on the cost function. The second observation is related to the optimization process, which must be defined as so fast it is possible, since, in a control application, the estimation must occur into the time between two samples.

The evaluation of both methods may be done with some metrics (Alessandri et al., 2008). One of them is the Root Mean Square Error, which defines if the variables are quite equal in all time instants, for n simulations. It is defined also the Asymptotic Root Mean Square Error (ARMSE), which measure the RMSE on the final window of time S, considering T the final simulation time.

$$RMSE(t) = \left(\sum_{i=1}^{n} \frac{\|e(t,i)\|^2}{n}\right)^{1/2} \qquad (31)$$

$$ARMSE = \sum_{T-S}^{T} \frac{1}{S+1}\left(\sum_{i=1}^{n} \frac{\|e(t,i)\|^2}{n}\right)^{1/2} \qquad (32)$$

4. SIMULATION AND STATE ESTIMATION

The quarter-car model is simulated with parameters of a typical passenger vehicle, moving on dry asphalt. To evaluate the system and the estimators, its dynamics is simulated considering an input torque defined with a proportional control law, so that the vehicle reaches a reference speed of 20 m/s. Then:

$$T = k_p\left(v_{ref} - v\right) \qquad (33)$$

Considering this condition, the input torque considered on the simulated system is presented on Figure 3.

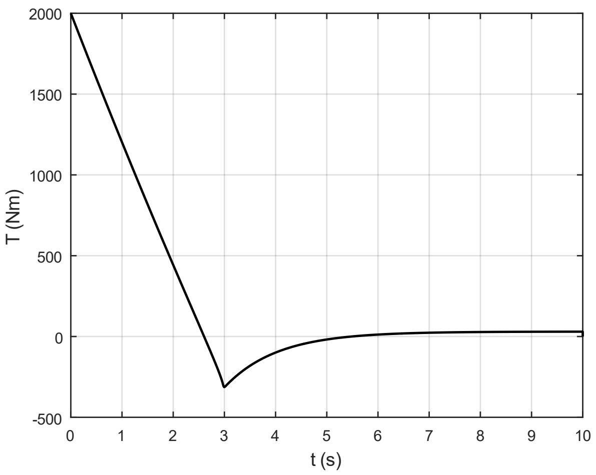

Figure 3: Input torque (Nm)

On the simulations, it is considered that output variable, that is the wheel rotation, is measured with different amplitude noises (ξ_n). So, the main objective of the estimators is to obtain the states along the time, based on this measured one. Evidently, as the system is full observable, when no noise is considered on the measurement devices, the states are precisely estimated. We must remark that, for EKF, this precision depends on the sample time adopted on discretization process and are close to zero, since the Jacobians have discontinuities. For MHSE, in this situation, the RMSE is equal zero.

In a second scenario, in which it is supposed that the measurement noise (ξ_n) has normal distribution with standard deviation of 1%, we have the results presented on the Figure 4 and Figure 5. In this situation, the input torque previously presented is applied on the wheel. It is possible to observe that it is suitable to reach a constant velocity, even with a steady-state error, which is no focus on this paper. The most important result we may remark is that the non-measured variables are estimated with good accuracy.

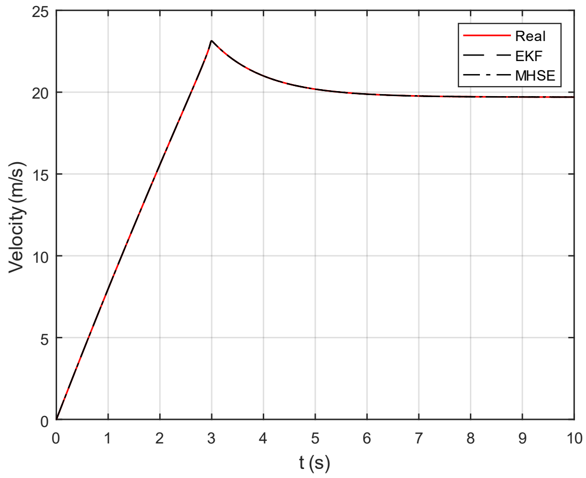

Figure 4: Estimated longitudinal velocity (m/s)

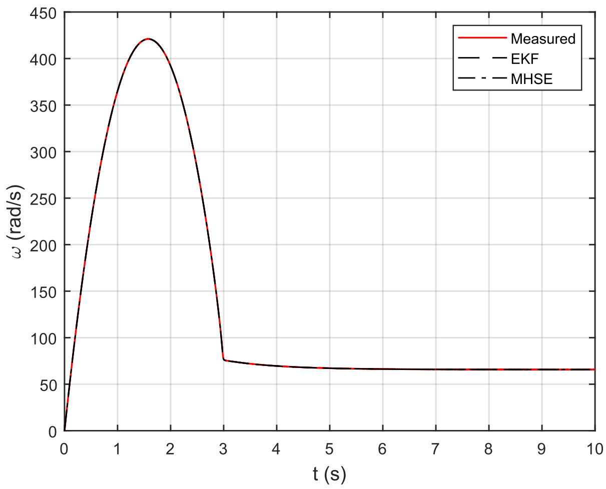

Figure 5: Estimated wheel rotation (rad/s)

For the simulation above, in which the initial conditions are well-known and the wheel rotation is measured with a noise of 1%, RMSE is presented on Table 1.

Table 1: RMSE results with well-known initial conditions

State	EKF	MHSE	Reduction
λ	0.0615	0.0025	95.935 %
v	0.0210	0.0023	89.048 %

We must do two remarks about these results. The first one is related to slip estimation. As there is no relation between the definition of input torque and slip, the initial values of longitudinal slip are very high, which represents the situation of the wheel slipping on the road. This may be observed on Figure 4, since the wheel rotation rises so quickly. In a second phase, the rotation falls, reducing the longitudinal slip to values between 0 and 1. The second remark is related to the Jacobians. The state equation related to the longitudinal slip presents many discontinuities points, mainly related to situations in which the velocity is zero. In this way, when this state is very low, the Jacobian F presents high values, harming the estimation process and also compromising the convergence. To prevent this situation, the same constraints applied to state variables are applied during estimation process. As the MHSE does not depend on derivatives, it is not affected by this situation and, so, its results are much better, presenting high relative reductions on RMSE. Figure 6 presents the estimated longitudinal slip in a converged simulation. It is important to remark that the states are estimated based on a noisy signal and compared with the supposed real one, which is noiseless. It is remarkable also the nearest values presented by the MSHE result (Figure 7).

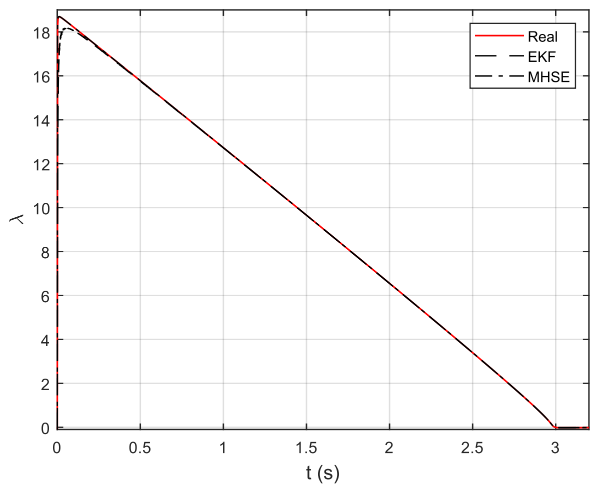

Figure 6: Estimated longitudinal slip.

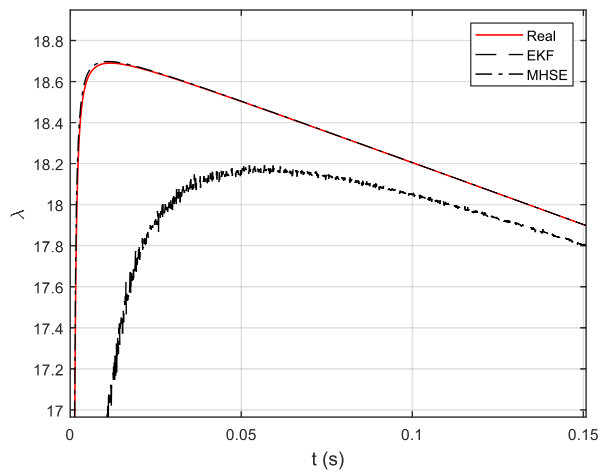

Figure 7: Estimated longitudinal slip, in detail.

In other analysis, we may realize the estimation process with different initial conditions, defined by uniformly distributed random numbers on interval [0,1], many times. This way, it is possible to observe its tendency in more sampled data and to verify if the estimators are capable to correct states even if the initial conditions are badly defined or unknown.

Table 2 presents the evaluation of the mean and the standard deviation of the ARMSE for longitudinal slip (λ), which is one of the non-measured states and is used on control strategies. In this table are presented the simulation results for different noise standard deviations, after the convergence of RMSE(t), briefly defined as ARMSE (equation (32)).

Table 2: ARMSE analysis for longitudinal slip (λ) estimation

Algorithm		EKF	MHSE
$\xi_n = 0.001$	Mean	0.0084	4.8188e-5
	St. Dev.	4.5271e-5	2.4763e-5
$\xi_n = 0.01$	Mean	0.4275	5.1430e-4
	St. Dev.	0.0043	2.9450e-4
$\xi_n = 0.05$	Mean	2.7254	0.0027
	St. Dev.	0.0363	0.0016

A more detailed analysis may be done interpreting the RMSE(t), as defined by equation (31), and that is presented on Figure 8, Figure 9 and Figure 10 for, respectively, standard deviations of 0.001, 0.01 and 0.05 on the measure noise.

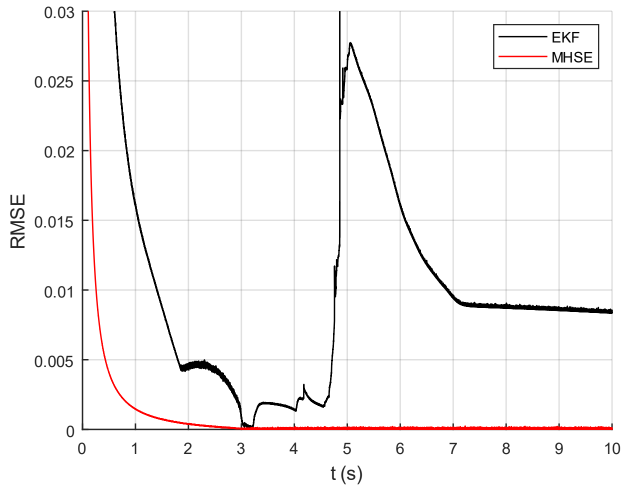

Figure 8: RMSE(t) for measurement noise of 0.1%

On the first scenario, it may be noted that in both methods the values of errors are larger in the initial samples, because it is supposed that the initial conditions are unknown and are treated as different to zero, when they really have this value on the simulation for data obtaining. Then, the RMSEs fall and converge for both algorithms, but for the MHSE, the value is lower than for EKF, denoting that the first one has a better accuracy. Besides that, the MHSE converges more quickly than EKF. In this way, we may affirm that the MHSE corrects badly defined initial conditions better than EKF. The last one presents an irregular behavior, with high variation before converging and even the final value is higher than MHSE one.

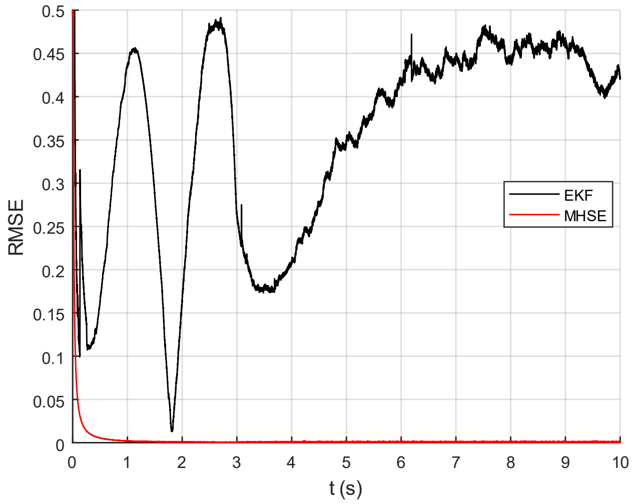

Figure 9: RMSE(t) for measurement noise of 1%

On the second scenario, the convergence occurs in the same configuration, that is, both converges, but MHSE converge to lower values in shorter times compared to EKF. Besides that, we may observe that the converged value of EKF is higher than the first case. The same aspect is observed on the last scenario (Figure 10).

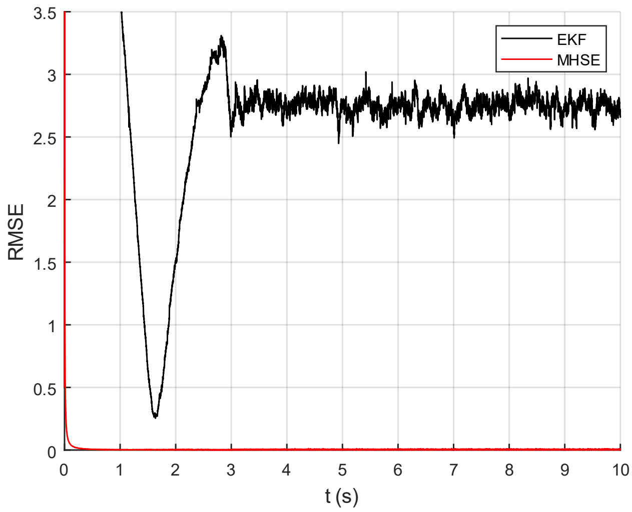

Figure 10: RMSE(t) for measurement noise of 5%

For the velocity estimation, the results are presented on Table 3. The results are similar to the longitudinal slip, which also demonstrates that MHSE has better performance in comparison to EKF.

In a general way, EKF do not present good results, when compared to MHSE in nonlinear mechanical systems. It may be noted that EKF is strongly affected by measurement noises, presenting a RMSE on the converged region higher than MHSE, mainly due to discontinuities on state equations. The second method is more robust to discontinuities on Jacobians and state equation, and the errors and time to convergence presented are lower. So, we may conclude about the higher performance of MHSE on nonlinear mechanical systems with discontinuities, as friction efforts.

Table 3: ARMSE analysis for velocity (v) estimation

Algorithm		EKF	MHSE
$\xi_n = 0.001$	Mean	0.9756	0.0014
	St. Dev.	0.0041	7.2911e-4
$\xi_n = 0.01$	Mean	3.8729	0.0147
	St. Dev.	0.0154	0.0083
$\xi_n = 0.05$	Mean	14.3821	0.0788
	St. Dev.	0.0491	0.0478

5. CONCLUSIONS

We may conclude about the efficiency of the MHSE in comparison to EKF on state estimation for nonlinear applications, especially with friction and discontinue efforts. In the studied case, both algorithms estimate the non-measured states. However, in a performance analysis, the MHSE presents better results, especially when it is considered the measurement errors and uncertainties in initial conditions of the system.

In future works, it is suggested the application of the estimation algorithm in complete vehicle models, considering all wheels and its lateral dynamics, in which it is possible to evaluate the estimator behavior on different maneuvers. In this sense, all tire longitudinal slip must be accurately estimated, which possibilities suitable control strategies for agile and high-speed path tracking.

Other future possible work is the definition of more complex control strategies with the objective of achieving prescribed velocities with optimized longitudinal slip. We must remark that in autonomous vehicle applications, state observers allow the possibility to define suitable controller for path tracking, agility, or stability.

It is also suggested the application of the developed estimators in other mechanical applications in which the friction efforts must be mitigated or estimated properly, especially on discontinuous systems, as, for example, with Coulomb friction, in which MHSE must present better performance compared to Kalman Filter approaches, since it is robustness demonstrated on the results section.

REFERENCES

Alessandri, A., Baglietto, M., & Battistelli, G. (2008). Moving-horizon state estimation for nonlinear discrete-time systems: New stability results and approximation schemes. *Automatica*, 44(7), 1753-1765.

Bar-Shalom, Y., Li, X. R., & Kirubarajan, T. (2004). *Estimation with applications to tracking and* *navigation: theory algorithms and software*. John Wiley & Sons.

Boada, B. L., Garcia-Pozuelo, D., Boada, M. J. L., & Diaz, V. (2016). A constrained dual Kalman filter based on pdf truncation for estimation of vehicle parameters and road bank angle: Analysis and experimental validation. *IEEE Transactions on Intelligent Transportation Systems*, *18*(4), 1006-1016.

Brembeck, J. (2019). Nonlinear constrained moving horizon estimation applied to vehicle position estimation. *Sensors*, *19*(10), 2276.

Chen, Y., & Wang, J. (2011). Adaptive vehicle speed control with input injections for longitudinal motion independent road frictional condition estimation. *IEEE Transactions on Vehicular Technology*, *60*(3), 839-848.

Du, H., Lam, J., Cheung, K. C., Li, W., & Zhang, N. (2015). Side-slip angle estimation and stability control for a vehicle with a non-linear tyre model and a varying speed. *Proceedings of the Institution of Mechanical Engineers, Part D: Journal of Automobile Engineering*, *229*(4), 486-505.

Feng, Y., Chen, H., Zhao, H., & Zhou, H. (2020). Road tire friction coefficient estimation for four wheel drive electric vehicle based on moving optimal estimation strategy. *Mechanical Systems and Signal Processing*, *139*, 106416.

Heidfeld, H., Schünemann, M., & Kasper, R. (2019). UKF-based State and tire slip estimation for a 4WD electric vehicle. *Vehicle System Dynamics*, 1-18.

Hong, S., Lee, C., Borrelli, F., & Hedrick, J. K. (2014). A novel approach for vehicle inertial parameter identification using a dual Kalman filter. *IEEE Transactions on Intelligent Transportation Systems*, *16*(1), 151-161.

Hsiao, T. (2012). Robust estimation and control of tire traction forces. *IEEE transactions on vehicular technology*, *62*(3), 1378-1383.

Hsu, Y. H. J., Laws, S. M., & Gerdes, J. C. (2009). Estimation of tire slip angle and friction limits using steering torque. *IEEE Transactions on Control Systems Technology*, *18*(4), 896-907.

Jalali, M., Hashemi, E., Khajepour, A., Chen, S. K., & Litkouhi, B. (2017). Integrated model predictive control and velocity estimation of electric vehicles. *Mechatronics*, *46*, 84-100.

Jazar, R. N. (2017). Driveline Dynamics. In *Vehicle Dynamics* (pp. 173-223). Springer, Cham.

Jeon, S. Y., Chung, R., & Lee, D. (2018, October). Tire Force Estimation of Dynamic Wheeled Mobile Robots using Tire-Model Based Constrained Kalman Filtering. In *2018 IEEE/RSJ International Conference on Intelligent Robots and Systems (IROS)* (pp. 2470-2477). IEEE.

Jo, K., Lee, M., & Sunwoo, M. (2015). Road slope aided vehicle position estimation system based on sensor fusion of GPS and automotive onboard sensors. *IEEE Transactions on Intelligent Transportation Systems*, *17*(1), 250-263.

Katriniok, A., & Abel, D. (2015). Adaptive EKF-based vehicle state estimation with online assessment of local observability. *IEEE Transactions on Control Systems Technology*, *24*(4), 1368-1381.

Kayacan, E., Young, S. N., Peschel, J. M., & Chowdhary, G. (2018). High-precision control of tracked field robots in the presence of unknown traction coefficients. *Journal of Field Robotics*, *35*(7), 1050-1062.

Kou, S. R., Elliott, D. L., & Tarn, T. J. (1973). Observability of nonlinear systems. *Information and Control*, 22(1), 89-99.

Li, B., Du, H., Li, W., & Zhang, B. (2019). Non-linear tyre model–based non-singular terminal sliding mode observer for vehicle velocity and side-slip angle estimation. *Proceedings of the Institution of Mechanical Engineers, Part D: Journal of automobile engineering*, *233*(1), 38-54.

Li, L., Jia, G., Ran, X., Song, J., & Wu, K. (2014). A variable structure extended Kalman filter for vehicle sideslip angle estimation on a low friction road. *Vehicle System Dynamics*, *52*(2), 280-308.

Lopes, E. D. R., Pinto, A. F. A., Valentim, M. X. G., Peixoto, P. S., & Neto, R. T. D. C. (2019). Extended model for calculation of soil-wheel contact area parameters in rigid soil-deformable tyre approximation. *International Journal of Vehicle Systems Modelling and Testing*, *13*(4), 358-372.

Na, J., Chen, A. S., Herrmann, G., Burke, R., & Brace, C. (2017). Vehicle engine torque estimation via unknown input observer and adaptive parameter estimation. *IEEE Transactions on Vehicular Technology*, *67*(1), 409-422.

Nilsson, J., Fredriksson, J., & Ödblom, A. C. (2014). Reliable vehicle pose estimation using vision and a single-track model. *IEEE Transactions on Intelligent Transportation Systems*, *15*(6), 2630-2643.

Pacejka, H. B., & Bakker, E. (1992). The magic formula tyre model. *Vehicle system dynamics*, *21*(S1), 1-18.

Savaresi, S. M., Tanelli, M., Cantoni, C., Charalambakis, D., Previdi, F., & Bittanti, S. (2005). Slip-deceleration control in anti-lock braking systems. *IFAC Proceedings Volumes*, *38*(1), 103-108.

Singh, K. B., Ali Arat, M., & Taheri, S. (2013). An intelligent tire based tire-road friction estimation technique and adaptive wheel slip controller for antilock brake system. *Journal of Dynamic Systems, Measurement, and Control*, *135*(3).

Sun, F., Lolenko, K., & Rudolph, J. (2014). Nonlinear observer design for state estimation during antilock braking. *Proceedings of the Institution of Mechanical Engineers, Part I: Journal of Systems and Control Engineering*, *228*(2), 78-86.

Zareian, A., Azadi, S., & Kazemi, R. (2016). Estimation of road friction coefficient using extended Kalman filter, recursive least square, and neural network. *Proceedings of the Institution of Mechanical Engineers, Part K: Journal of Multi-body Dynamics*, *230*(1), 52-68.

Zhao, L., & Liu, Z. (2014). Vehicle velocity and roll angle estimation with road and friction adaptation for four-wheel independent drive electric vehicle. *Mathematical Problems in Engineering*, *2014*.